Discrete Green's Function Formulation of the FDTD Method and Its Application in Antenna Modeling

Weili Ma, Mark R. Rayner, *Member, IEEE*, and Clive G. Parini, *Member, IEEE*

***Abstract*—A discrete Green's function formulation of the finite-difference time-domain (DGF-FDTD) method based on both discrete system theory and the FDTD method has been developed, which expresses the field response as a convolution of current sources and the impulse response of the FDTD equation system. The DGF-FDTD method presents the FDTD equations in a different perspective from the conventional Yee algorithm. It avoids the computational difficulties such as the need for computation of free-space nodes and absorbing boundary conditions of the classic FDTD method. The ability of the DGF-FDTD method to model on antenna is demonstrated by the modeling of a Yagi–Uda array antenna with considerable saving in memory usage.**

***Index Terms*—Absorbing boundary condition (ABC), discrete Green's function (DGF), finite-difference time-domain (FDTD) method.**

I. Introduction

THE finite-difference time-domain (FDTD) method [1] is a robust, powerful, and popular general method to solve Maxwell's partial differential equations numerically in the time domain. It has been used extensively to model all kinds of electromagnetic problems such as radiation, scattering, and circuit problems. However, due to the limitation of computer resources, it is usually difficult to apply the FDTD method in the modeling of electrically large objects, especially when applied to problems with large spacing between objects. The improvements in modern computer technology have made this difficulty less serious, but the inherent features of the classic FDTD method still impose some difficulties when dealing with electrically large objects. First, the implementation of the FDTD method requires absorbing boundary conditions to terminate the spatial computational grid. Moreover, the recursive nature of the classic Yee algorithm [2] for the FDTD method implies that all the cells contained in a given volume must be computed, which means a great deal of computational time and computer memory is dedicated to determining free space fields between objects which are actually of little interest. As a result, the FDTD method is characteristically time consuming and memory demanding.

To improve the efficiency and accuracy of the FDTD method and make its application in electrically large objects more practical, researchers have proposed various methods [3], [4]. In this paper, the discrete Green's function formulation of the FDTD method (DGF-FDTD) was developed to examine the FDTD method from a system point of view [5]. The DGF-FDTD method is based on the idea that the Yee algorithm may not be the only possible formulation of the FDTD method. Classic theory of discrete systems [6] shows that any linear and invariant system can be completely determined by the impulse response of the system. This is the discrete version of the Green's function technique [7] extensively used in electromagnetics. This DGF formulation of the FDTD method solve for the FDTD equations without the need for absorbing boundary conditions (ABCs) or the computation of free-space nodes. For the practical implementation of the algorithm, the analytical formula of the impulse response or the discrete Green's function of the FDTD system must be known. This paper discusses in detail the derivation of the analytical form of the discrete Green's function in the one-, two-, and three-dimensional cases and its application in antenna modeling and as an ABC.

Manuscript received December 18, 2002; revised December 20, 2003.

The authors are with the Queen Mary University of London, London E1 4NS, U.K. (e-mail: c.g.parini@elec.qmul.ac.uk).

Digital Object Identifier 10.1109/TAP.2004.838797

II. Discrete Green's Function Formulation of the FDTD Method

A. FDTD Equations as a Discrete System and Its Z-Domain Representation

The FDTD equations can be treated as a linear and invariant discrete system whose "inputs" are the electric and magnetic current density sources $\vec{J}$ and $\vec{M}$, respectively, and the "outputs" are the electric and magnetic fields $\vec{E}$ and $\vec{H}$. The impulse response of the FDTD equations can be determined by using the Kronecker delta function as the excitation. This gives a set of 2×2 matrices, which is the Green's function of the FDTD system. The response to an arbitrary source is then expressed as the convolution of the source with the Green's function. The full procedure for the derivation of the discrete Green's function will be described in this paper.

The impulse response of a system is usually more easily obtained in the spectral domain, which is then inverse transformed back into the real domain. The Z-transform is a powerful tool widely used in the analysis of discrete systems [6], [8]. Throughout this paper, the unilateral Z-transform will be used since the FDTD system is a causal system. When the FDTD equations are represented in the Z-domain a four-dimensional Z-transform with four complex variables in the Z-domain is required $(n, i, j, k) \stackrel{z}{\rightarrow} (\Omega, X, Y, Z)$. Starting with the simplest case is the FDTD equations for the linear, isotropic, nondispersive, and lossless free-space media. Let us take the E_x component of the electric field as an example. The FDTD equation for E_x has half space and time step components, but in

computation it is necessary to omit the term 1/2 in the indexes, which results in the FDTD equation with integer indexes (1)

$$E_x^n(i,j,k) = E_x^{n-1}(i,j,k) + \frac{\Delta t}{\varepsilon} \times \left(\frac{H_z^{n-1}(i,j+1,k) - H_z^{n-1}(i,j,k)}{\Delta y} - \frac{H_y^{n-1}(i,j,k+1) - H_y^{n-1}(i,j,k)}{\Delta z} - j_x^n(i,j,k) \right). \quad (1)$$

Using the definitions of Z-transform and its property and defining $D_\Omega = (\Omega - 1)/\Delta t$, $D_Y = (Y - 1)/\Delta y$, $D_Z = (Z - 1)/\Delta z$, (1) can be written as

$$E_z(\Omega,X,Y,Z) = \frac{D_\Omega^{-1}}{\varepsilon} \left(D_Y H_z(\Omega,X,Y,Z) - D_Z H_y(\Omega,X,Y,Z) - J_z(\Omega,X,Y,Z) \right). \quad (2)$$

Similarly, the Z-domain representations of the E_y and E_z components can be obtained. For the magnetic field, let us take H_z as an example. It is noted that H_z is taken 1/2 time step later than the E_x component. Therefore, for the time step, it is necessary to keep the integer in the electric field and omit the half time step in the magnetic field. It is now possible to obtain the Z-domain representation of H_z (3)

$$H_z(\Omega,X,Y,Z) = \frac{\Omega D_\Omega^{-1}}{\mu} \left(Y^{-1} D_Y E_x(\Omega,X,Y,Z) - X^{-1} D_X E_y(\Omega,X,Y,Z) - M_z(\Omega,X,Y,Z) \right). \quad (3)$$

The Z-domain representations of H_x and H_y are obtained in a similar fashion. The three components of both the electric and magnetic fields can be written in a matrix form in the Z-domain (4), (5)

$$\vec{E}(\Omega,X,Y,Z) = \frac{D_\Omega^{-1}}{\varepsilon} \left(A_e \cdot \vec{H}(\Omega,X,Y,Z) - \vec{J}(\Omega,X,Y,Z) \right)$$

$$A_e = \begin{pmatrix} 0 & -D_Z & D_Y \\ D_Z & 0 & -D_X \\ -D_Y & D_X & 0 \end{pmatrix} \quad (4)$$

$$\vec{H}(\Omega,X,Y,Z) = \frac{\Omega \cdot D_\Omega^{-1}}{\varepsilon} \times \left(A_h \cdot \vec{E}(\Omega,X,Y,Z) - \vec{M}(\Omega,X,Y,Z) \right)$$

$$A_h = \begin{pmatrix} 0 & Z^{-1} D_Z & -Y^{-1} D_Y \\ -Z^{-1} D_Z & 0 & X^{-1} D_X \\ Y^{-1} D_Y & -X^{-1} D_X & 0 \end{pmatrix}. \quad (5)$$

B. Z-Domain Finite-Difference Second-Order Vector Wave Equation and Its Relationship With the Scalar Wave Equation

For the continuous case, the second-order vector wave equation can be obtained from the two Maxwell's curl equations. Similarly, the Z-domain finite-difference second-order equation can be obtained by substituting the electric field equation into the magnetic field equation and vice versa [9]. The Z-domain expression of the finite-difference vector equation for the electric field is obtained by substituting (5) into (4), yielding (6) as shown at the bottom of the page, where I is Kronecker delta function.

This formulation of the discrete vector wave equation for the electric field (6) is given in the Z-domain but can be easily transformed to the real domain by taking the D-terms as finite-difference operators and can be compared to the continuous vector wave equation. The solution to the discrete vector wave equation is fully compatible with the FDTD system since the former is deduced from the latter without any additional conditions applied.

When the vector wave equation is source free, in the continuous case it can be reduced to the scalar wave equation. This equation also has a discrete version in terms of the second-order finite differences in the Z-domain

$$\left(\Omega^{-1} \cdot \frac{D_\Omega^2}{c^2} - \left(X^{-1} \cdot D_X^2 + Y^{-1} \cdot D_Y^2 + Z^{-1} \cdot D_Z^2 \right) \right) \cdot \Phi = 0. \quad (7)$$

In order to obtain the relationship between the discrete vector and scalar wave equations it is necessary to use the "divergence" equation and the continuity condition of current. These two equations together provide an additional relationship between the electric field and the current which can be used to simplify the electric finite difference vector wave equation (6) and make the coefficient matrix diagonal, yielding

$$\left(\Omega^{-1} \cdot \frac{D_\Omega^2}{c^2} - \left(X^{-1} \cdot D_X^2 + Y^{-1} \cdot D_Y^2 + Z^{-1} \cdot D_Z^2 \right) \right) \cdot \vec{E} = -\mu D_\Omega \left(\Omega^{-1} \vec{I} - c^2 D_\Omega^{-2} \vec{D}_1 \vec{D}_2 \right) \cdot \vec{J} - A_e \vec{M}$$

$$\vec{D}_1 = X^{-1} \cdot D_X \hat{x} + Y^{-1} \cdot D_Y \hat{y} + Z^{-1} \cdot D_Z \hat{z}$$

$$\vec{D}_2 = D_X \hat{x} + D_Y \hat{y} + D_Z \hat{z}. \quad (8)$$

The solution to (8) should be exactly the same as the solution of the FDTD equations to the electric field with same initial conditions. When there are no excitation currents, the vector wave equation reduces to three scalar wave equations which have a

$$\left(\frac{\Omega^{-1} D_\Omega^2}{c^2} \cdot \vec{I} - A_e \cdot A_h \right) \cdot \vec{E} = \Omega^{-1} D_\Omega \mu \cdot \vec{J} + A_e \cdot \vec{M}$$

$$A_e \cdot A_h = \begin{pmatrix} Y^{-1} D_Y^2 + Z^{-1} D_Z^2 & -X^{-1} D_X D_Y & -X^{-1} D_X D_Z \\ -Y^{-1} D_X D_Y & X^{-1} D_X^2 + Z^{-1} D_Z^2 & -Y^{-1} D_Y D_Z \\ -Z^{-1} D_X D_Z & -Z^{-1} D_Y D_Z & X^{-1} D_X^2 + Y^{-1} D_Y^2 \end{pmatrix} \quad (6)$$

solution only when the values of the complex parameters in the Z-domain cancel the scalar wave operator (9)

$$\Omega^{-1}\cdot\frac{D_\Omega^2}{c^2}-\left(X^{-1}\cdot D_X^2+Y^{-1}\cdot D_Y^2+Z^{-1}\cdot D_Z^2\right)=0. \quad (9)$$

This is actually the dispersion formula for the discrete FDTD system. This expression is similar to the formulation of $k^2-(k_x^2+k_y^2+k_z^2)=0$ of the continuous case. Equation (9) shows the relationship for the complete complex plane. In the particular case of the unit circle of the complex plane, (9) becomes the normal formula of dispersion (10)

$$\begin{aligned}\frac{1}{c^2\Delta t^2}\sin^2\left(\frac{\omega\Delta t}{2}\right)&=\frac{1}{\Delta x^2}\sin^2\left(\frac{k_x\Delta x}{2}\right)\\&+\frac{1}{\Delta y^2}\sin^2\left(\frac{k_y\Delta y}{2}\right)+\frac{1}{\Delta z^2}\sin^2\left(\frac{k_z\Delta z}{2}\right)\\ \Omega=e^{j\omega\Delta t},\ X=e^{jk_x\Delta x},&Y=e^{jk_y\Delta y},\ Z=e^{jk_z\Delta z}. \quad (10)\end{aligned}$$

It is then seen that the dispersion relationship is inherently included in the Z-domain formulation of the FDTD equations.

C. Solutions to the Finite-Difference Wave Equations

To get the impulse response to the scalar wave equation, it is necessary to excite the system with a delta function. Taking a shifted Kronecker delta as the excitation, its real and Z-domain representations are

$$\begin{aligned}\delta_{i-i'j-j'k-k'}^{n-n'}&=\delta(n-n')\delta(i-i')\delta(j-j')\delta(k-k')\\ Z\left(\delta_{i-i'j-j'k-k'}^{n-n'}\right)&=\Omega^{-n'}X^{-i'}Y^{-j'}Z^{-k'}. \quad (11)\end{aligned}$$

The impulse response to the scalar wave equation (12) can be obtained from the Z-domain representation of the scalar wave equation (7) and the excitation (11), which is just the ratio between the impulse excitation in the Z-domain and the "transfer function" of the scalar wave equation

$$\Gamma=\frac{\Omega^{-n'}\cdot X^{-i'}\cdot Y^{-j'}\cdot Z^{-k'}}{\Omega^{-1}\cdot\frac{D_\Omega^2}{c^2}-\left(X^{-1}\cdot D_X^2+Y^{-1}\cdot D_Y^2+Z^{-1}\cdot D_Z^2\right)}. \quad (12)$$

Equation (12) is in the Z-domain; however, the solution needs to be in the real domain. In continuous electromagnetics the Green's function of the scalar wave equation can be determined either by taking the inverse transform of the spectral domain representation or by direct integration of the equation in differential form. The mathematical solution is extremely simplified by using the spherical symmetry of the problem, and the Green's function problem can be reduced to a one-dimensional (1-D) problem in spherical coordinates. However, it is impossible to use the same spherical symmetry conditions in the discrete case since the discrete Cartesian grid is essentially not isotropic as continuous space–time is. Therefore, we choose to solve each coordinate contributing to the finite equations separately while taking the other coordinates as constants [10]. First, the scalar wave equation will be solved for the time index in the real domain. The Z-domain operator related to time is $\Omega^{-1}\cdot D_\Omega^2$, which can be easily transformed into real domain as $(\Phi^{n+1}-2\Phi^n+\Phi^{n-1})/\Delta t^2$, allowing (7) to be rewritten in the following form:

$$\Phi^{n+1}-2\Phi^n+\Phi^{n-1}=K\cdot\Phi^n$$

where

$$\begin{aligned}\Phi^n&=\Phi^n(X,Y,Z)\\ K&=c^2\Delta t^2\left(X^{-1}\cdot D_X^2+Y^{-1}\cdot D_Y^2+Z^{-1}\cdot D_Z^2\right). \quad (13)\end{aligned}$$

K is taken as a constant here since only the time index is solved in the real domain at this time. The complex exponential sequences (14) can be tested as a solution to (13) since they are eigenfunctions for any linear system

$$\Phi^n=C_1(X,Y,Z)e^{jn\omega\Delta t}+C_2(X,Y,Z)e^{-jn\omega\Delta t}. \quad (14)$$

The parameter of the complex exponential is obtained by direct substitution into (13). As a result the general solution of (13) is determined with $\varphi=1-K/2$

$$\Phi^n=C_1(X,Y,Z)e^{jn\arccos(\varphi)}+C_2(X,Y,Z)e^{-jn\arccos(\varphi)}. \quad (15)$$

For simplicity, (15) can be expressed in terms of Chebyshev polynomials (16)

$$\Phi^n=B_1(X,Y,Z)\cdot T_n(\varphi)+B_2(X,Y,Z)\cdot\sqrt{1-\varphi^2}\,U_{n-1}(\varphi) \quad (16)$$

where $B_1=C_1+C_2$; $B_2=j(C_1-C_2)$; $T_n(\varphi)=\cos(n\arccos(\varphi))$ (Chebyshev polynomial, first order) $U_n(\varphi)=\sin((n+1)\arccos(\varphi))/\sqrt{1-\varphi^2}$ (Chebyshev polynomial, second order).

The impulse response is a particular solution of the scalar wave equation when the excitation is a delta function. The constants C_1 and C_2 in the general solution to the homogeneous equation are determined by the initial condition of the problem. As a result the impulse response is now obtained, with the time index in the real domain and the spatial indexes remaining in the Z domain (17)

$$\begin{aligned}\Phi^{n+1}&=\Gamma^{n+1}(X,Y,Z)=U_n(\varphi)\\ B_1&=0\quad B_2=\frac{1}{\sqrt{1-\varphi^2}}. \quad (17)\end{aligned}$$

It is now necessary to determine the spatial indexes in the real domain as well. Equation (17) can be expanded as a power sum as follows:

$$\Gamma^{n+1}(X,Y,Z)=U_n(\varphi)=\sum_{m=0}^{\frac{n}{2}}(-1)^m\binom{n-m}{m}\cdot(2\varphi)^{n-2m}. \quad (18)$$

The inverse Z-transform for the spatial indexes can be obtained from the inverse Z-transform of all the $(2\varphi)^p(p=n-2m)$ terms, which have the spatial complex variable. For simplicity let us consider the 1-D case as an example.

D. Impulse Response for Scalar Wave Equation

For the 1-D case, the problem only considers the spatial index i. The operator φ is reduced to

$$2\varphi=2+K,\quad K=c^2X^{-1}D_X^2\Delta t^2. \quad (19)$$

TABLE I
THE 1-D DISCRETE GREEN'S FUNCTION AS A FUNCTION OF n

n	1	2	3	4	5
G_0^n (DGF)	0.10003019	0.50030210	0.49984915	0.87484881	0.87541499
G_0^n(time stepping)	0.10003019	0.50030209	0.49984915	0.87484881	0.87541498

The variable φ can be expressed as a product of X

$$2\varphi=\alpha X(X^{-1}-R_1)(X^{-1}-R_2)$$

where

$$\alpha=\frac{c^2\Delta t^2}{\Delta x^2},\quad \beta=\frac{\alpha-1}{\alpha}, R_{1,2}=\beta\pm\sqrt{\beta^2-1}, R_1R_2=1. \tag{20}$$

The inverse transform of the power terms can be obtained in a direct way by binomial expansion into simple powers of X. The binomial expansion of the $(X^{-1}-R_1)^p$ term takes the form of

$$(X^{-1}-R_1)^p=\sum_{i=0}^{p}\binom{p}{i}(-R_1)^{p-i}X^{-i}. \tag{21}$$

By using the definition of the Z-transform, the inverse Z-transform of $(X^{-1}-R_1)^p$ can be readily obtained (22)

$$(X^{-1}-R_1)^p\xrightarrow{z^{-1}}\binom{p}{i}(-R_1)^{p-i}. \tag{22}$$

The inverse Z-transform of the other two terms of (20) can be obtained in a similar way. As a result the inverse Z-transform of $(2\varphi)^p$ is found as

$$(2\varphi)^p\xrightarrow{z^{-1}}\alpha^p\sum_{i=0}^{p-i}\binom{p}{l}\binom{p}{l-i}(-R_2)^{p-l}(-R_1)^{l-i}. \tag{23}$$

The orthogonal Jacobi polynomials $J_n^{(\alpha,\beta)}(\xi)$ on the unit circle [11] have the form of

$$J_n^{(\alpha,\beta)}(\xi)=\frac{1}{2^n}\sum_{m=0}^{N}\binom{n+\alpha}{m}\binom{n+\beta}{n-m}(\xi-1)^{n-m}(\xi+1). \tag{24}$$

It can be seen that (23) can be identified as a Jacobi polynomial with an extra term $(R_2-R_1)^{(p-i)}$ (25) when i is taken as α, i as β, $p-i$ as n, $l-i$ as m, and $(R_1+R_2)/(R_1-R_2)$ as ξ

$$(2\varphi)^p\xrightarrow{z^{-1}}\alpha^p J_{p-i}^{(i,i)}(\xi)\cdot(R_2-R_1)^{p-i}. \tag{25}$$

The impulse response of the 1-D scalar wave equation is now determined as the polynomial of the grid parameters given in (20), which is achieved by introducing (25) into (18). The resulting 1-D impulse response for the finite-difference scalar wave equation is given as

$$g_i^{n+1}=\sum_{m=0}^{\frac{n}{2}}(-1)^m\binom{n-m}{m}\cdot\alpha^{n-2m}\cdot J_{n-i-2m}^{(i,i)}(\xi)\cdot(R_2-R_1)^{n-i-2m}. \tag{26}$$

The analytical form of the two-dimensional (2-D) (27) and three-dimensional (3-D) (28) discrete Green's function can be obtained by the same method as for the 1-D case

$$\begin{aligned}g_{i,j}^{n+1}=&\sum_{m=0}^{\frac{n}{2}}(-1)^m\binom{n-m}{m}\cdot\sum(n-2m;p_x,p_y)\\&\cdot\alpha_x^{p_x}J_{p_x-i}^{(i,i)}(\xi_x)(R_{2x}-R_{1x})^{p_x}\\&\cdot\alpha_y^{p_y}J_{p_y-j}^{(j,j)}(\xi_y)(R_{2y}-R_{1y})^{p_y}\end{aligned} \tag{27}$$

$$\begin{aligned}g_{i,j,k}^{n+1}=&\sum_{m=0}^{\frac{n}{2}}(-1)^m\binom{n-m}{m}\cdot\sum(n-2m;p_x,p_y,p_z)\\&\cdot\prod_{\substack{l=i,j,k\\s=x,y,z}}\alpha_s^{p_s}J_{p_s-l}^{(l,l)}(\xi_s)(R_{2s}-R_{1s})^{p_s-l}\end{aligned} \tag{28}$$

where

$$\begin{aligned}\alpha_s&=\frac{c^2\Delta t^2}{\Delta s^2}\frac{(\Delta x^2+\Delta y^2+\Delta z^2)}{\Delta s^2},\beta_s=\frac{\alpha_s-1}{\alpha_s}\\R_{1s}&=\beta_s+\sqrt{\beta_s^2-1},R_{2s}=\beta_s-\sqrt{\beta_s^2-1}\\\xi_s&=\frac{R_{1s}+R_{2s}}{R_{1s}-R_{2s}},s=x,y(,z)\\(p_z+p_y+p_z)&=n-2m\\(n-2m;p_x,p_y,p_z)&=\frac{(n-2m)!}{p_x!p_y!p_z!}.\end{aligned} \tag{29}$$

The impulse response in the multidimensional case is not simply a discrete version of the Green's function for the continuous equation. The impulse response reflects the basic properties of the discrete grid such as dispersion and anisotropy that do not happen for the continuous coordinate. The impulse excitation contains all the frequencies allowed in the discrete grid. For some frequencies Δx is close to $\lambda/2$. In this case, the wave propagation in the numerical FDTD grid shows very strong dispersion.

E. Numerical Evaluation of the Discrete Green's Function

The discrete Green's function obtained previously is of analytical form; it is a function of both spatial and temporal steps Δx and Δt. Let us now discuss the numerical evaluation of the discrete Green's function. For the 1-D DGF, if the delta function is applied at the spatial index $i=0$, the DGF computed at this point against time can be obtained, which gives the Green's function as a function of α. When $\alpha=0.5$, the first few terms of the 1-D Green's function take the values of Table I. This Green's function can also be obtained through a time-stepping numerical procedure. The result from the time-stepping algorithm for a same grid is also listed in Table I for comparison.

It is seen that difference between the numerical and analytical calculation of the Green's function lies in the seventh decimal

place. Since both results are an exact solution to the same finite difference problems, they should be the same. The tiny difference here is basically due to the finite precision of the floating point representation of real number in the computer.

Another example is given for a 2-D 60×60 grid. The grid is excited at the center point $i = 30$, $j = 30$, with spatial and time parameters $\Delta x = \Delta y = 0.15$, $c\Delta t = 0.632$. Fig. 1 is the contour graph of the 2-D discrete Green's function over the whole grid at time step $t = 20$ and $t = 30$, respectively. The anisotropy and causality of the Green's function can be observed from the graph.

F. Impulse Response to the Vector Wave Equation: Z-Domain Representation

The vector wave equation can be reduced to the scalar wave equation for the electromagnetic fields in both the discrete and continuous cases. Therefore, the Green's function for the vector wave equation can be directly related to the Green's function for the scalar equation by applying the operator to the scalar Green's function. The impulse response to the discrete vector wave equation in the Z-domain can also be determined from the scalar impulse response in the Z-domain in a similar way, yielding

$$\vec{\Gamma}^n_{i,j,k} = (\Xi \cdot \hat{j} + \Lambda \cdot \hat{m}) \cdot \Gamma^n_{i,j,k} \tag{30}$$

where $\vec{\Gamma}^n_{i,j,k}$ is vector impulse response and $\Gamma^n_{i,j,k}$ is scalar impulse response.

Expanding the finite-difference operator for the current source of (30) in a matrix form gives (31) as shown at the bottom of the page.

This operator establishes a link between the vector and scalar Green's function in the Z-domain. It is also the Green's function linking the electric current and electric field; therefore, it is designated as G_{ej}. Other Green's functions are named in the same fashion. The time-domain vector Green's function takes the form of a matrix and its relationship with the time-domain scalar Green's function can be found through translating the finite-difference operators in the Z-domain into time-domain finite-difference operators. Take the first element of the matrix of (31) as an example (ignoring the constant μ for the purpose of simplicity). Its real domain form can be obtained by applying the inverse Z-transform to the corresponding variables (32)

$$[G_{ej}]_{xx} = g^n_{i,j,k} - g^{n-1}_{i,j,k} - \alpha_x \sum_{l=0}^{n} -g^{n-1}_{i-1,j,k} - 2g^{n-1}_{i,j,k} + g^{n-1}_{i+1,j,k}. \tag{32}$$

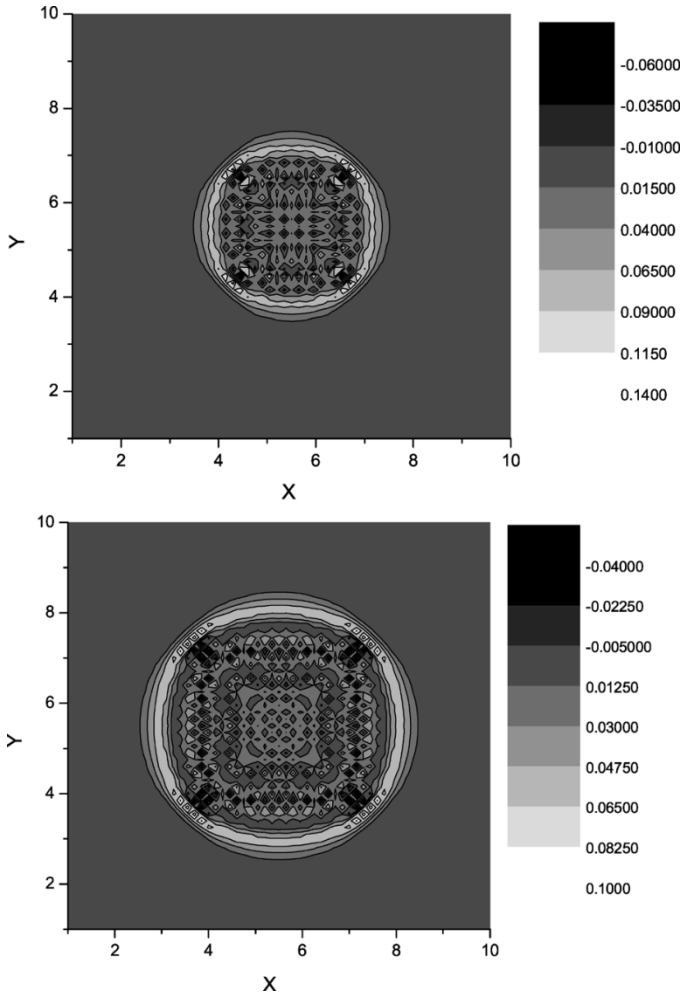

Fig. 1. Contour graph of 2-D discrete Green's function at $t = 20$ and $t = 30$, respectively.

All the other elements can be inverse Z-transformed similarly to obtain the other components of the vector Green's function, which will not be listed here for the purpose of simplicity. Other matrices such as G_{em}, G_{hj} and G_{hm} can be determined in a similar fashion, which will not be explored in detail here.

G. FDTD Equations Formulated as a Convolution of the Green's Function and the Current Sources

The impulse response of the FDTD equations can be determined with Kronecker delta impulse functions as sources. It is a set of 2×2 matrices (33), which represent the $\vec{E}$ and $\vec{H}$ fields

$$\begin{aligned} \Xi \cdot &= -\mu D_\Omega \left(\Omega^{-1} \bar{I} - c^2 D_\Omega^{-2} \vec{D}_1 \, \vec{D}_2 \right) \\ &= -\mu \begin{bmatrix} \Omega^{-1} D_\Omega - c^2 D_\Omega^{-1} X^{-1} D_X^2 & -c^2 D_\Omega^{-1} X^{-1} D_X D_Y & -c^2 D_\Omega^{-1} X^{-1} D_X D_Z \\ -c^2 D_\Omega^{-1} Y^{-1} D_X D_Y & \Omega^{-1} D_\Omega - c^2 D_\Omega^{-1} Y^{-1} D_Y^2 & -c^2 D_\Omega^{-1} Y^{-1} D_Y D_Z \\ -c^2 D_\Omega^{-1} Z^{-1} D_X D_Z & -c^2 D_\Omega^{-1} Z^{-1} D_Y D_Z & \Omega^{-1} D_\Omega - c^2 D_\Omega^{-1} Z^{-1} D_Z^2 \end{bmatrix} \end{aligned} \tag{31}$$

obtained when sources $\vec{J}$ and $\vec{M}$ are Kronecker delta functions with arbitrary unitary vectors $\hat{j}$ and $\hat{m}$ functions

$$\begin{pmatrix} \vec{E}_{imp} \\ \vec{H}_{imp} \end{pmatrix} = \begin{pmatrix} [G_{ej}]^n_{ijk} & [G_{em}]^n_{ijk} \\ [G_{hj}]^n_{ijk} & [G_{hm}]^n_{ijk} \end{pmatrix} \cdot \begin{pmatrix} \hat{j} \\ \hat{m} \end{pmatrix}. \quad (33)$$

For an arbitrary current density source, according to the discrete system theory, it can be expressed as a convolution sum of Kronecker delta functions. Therefore the field responses can be obtained as the convolution of the impulse response and the current density sources (34)

$$\begin{pmatrix} \vec{E}^n_{ijk} \\ \vec{H}^n_{ijk} \end{pmatrix} = \sum_{n'i'j'k'} \begin{pmatrix} [G_{ej}]^{n-n'}_{i-i'j-j'k-k'} & [G_{em}]^{n-n'}_{i-i'j-j'k-k'} \\ [G_{hj}]^{n-n'}_{i-i'j-j'k-k'} & [G_{hm}]^{n-n'}_{i-i'j-j'k-k'} \end{pmatrix} \cdot \begin{pmatrix} \vec{J}^{n'}_{i'j'k'} \\ \vec{M}^{n'}_{i'j'k'} \end{pmatrix}. \quad (34)$$

Equation (34) is referred to as the convolution formulation of the FDTD method. The impulse response is known as the discrete Green's function (DGF) of the FDTD system. It takes the form of a matrix and corresponds to the dyadic Green's function concept in continuous electromagnetics. Using the DGF method, the FDTD equations are implemented as a discrete convolution sum which produces exactly the same result as the Yee algorithm based on the finite-difference equations. Despite the fact that the DGF-FDTD is equivalent to the Yee algorithm, it does not require ABCs and only the currents on the scatterer need to be stored. The steps $\Delta x, \Delta y, \Delta z$, and Δt are the same as for the Yee algorithm in order to ensure stability and low dispersion. It will be demonstrated that the DGF-FDTD method can be separately used to solve antenna problems in the time domain and compute antenna parameters (antenna pattern, impedance). At the same time, the DGF-FDTD method can also work as a hybrid method with the FDTD method in electromagnetic modeling to eliminate some of the computational difficulties. The DGF-FDTD formulation can also work as an exact ABC for the Yee algorithm by employing the principle of equivalence. The next section will be dedicated to the investigation of the DGF's application.

III. Application of the DGF-FDTD Method in Antenna Modeling

A. The Applications of the DGF-FDTD Method

The convolution formulation of the FDTD (34) shows that the fields at a specific location on or around the structure of interest can be computed from the superposition of all the Green's functions and current sources on the structure. The knowledge of the analytical formulation of the discrete Green's function allows the calculation of the impulse response at certain single index positions without the need for absorbing boundary conditions. This is very significant, as it would permit the analytical determination of the exact FDTD response across a homogeneous region without the need for the calculation of the intermediate nodes.

As stated previously, the DGF formulation is derived from the FDTD equations directly without any other additional condition; thus the two methods can be combined perfectly without incurring any numerical errors or interface problems. The two methods can work together in dealing with electromagnetic problems, where the DGF is used for the analytical solution across a homogeneous domains while the FDTD method is used to solve in the adjacent inhomogeneous regions. At the same time, since the DGF method does not require the implementation of ABCs because it can determine the fields at any point just from the currents directly, it will work perfectly as an ABC for the Yee algorithm. The convolution formulation of the DGF method is used to compute the electric field on the boundary walls which will be further used to update the Yee algorithm. By this means DGF works as an ABC for the FDTD grid.

For the purpose of simplicity, the application of the DGF method as an ABC for Yee algorithm will not be discussed in this paper. The application of the DGF method in antenna modeling is presented as a demonstration of the convolution formulation of the FDTD method.

B. Scattering Formulation of the DGF-FDTD Method

In the FDTD grid, the boundary condition on the electric and magnetic conductors is satisfied by setting to zero the total tangential electric or magnetic field at the nodes which are filled with the electric or magnetic conductors [12]

$$\begin{aligned} \vec{E}_t &= \vec{E}_{\text{inc}} + \vec{E}_{\text{scat}} = 0 \; i,j,k, \in \text{electric conductor} \\ \vec{H}_t &= \vec{H}_{\text{inc}} + \vec{H}_{\text{scat}} = 0 \; i,j,k, \in \text{magnetic conductor.} \end{aligned} \quad (35)$$

Using the convolution formulation of the FDTD method (34), the scattered fields can be determined from the currents induced on the structure, which are then combined with the boundary condition to link mathematically the incident field to the currents induced on the scatterer.

Equation (36) has to be inverted so that the induced currents on the antenna are expressed as a function of the incident fields which will result in the following scattering (37). In (37), the current densities on the scatterer are related to the incident field at the same time instant and to the current densities at previous time steps. As a consequence, the induced currents can be solved for each time step through iteration of the currents previously calculated. The iteration starts from the time index $n = 0$ (before $n = 0$, the incident field and the currents are assumed to be zero) and ends at the time index N.

$$\begin{pmatrix} \vec{E}^n_{ijk} \\ \vec{H}^n_{ijk} \end{pmatrix}_{\text{inc}} + \sum_{n'i'j'k'} \begin{pmatrix} [G_{ej}]^{n-n'}_{i-i'j-j'k-k'} & [G_{em}]^{n-n'}_{i-i'j-j'k-k'} \\ [G_{hj}]^{n-n'}_{i-i'j-j'k-k'} & [G_{hm}]^{n-n'}_{i-i'j-j'k-k'} \end{pmatrix} \cdot \begin{pmatrix} \vec{J}^{n'}_{i'j'k'} \\ \vec{M}^{n'}_{i'j'k'} \end{pmatrix} = 0 \quad (36)$$

and

$$\begin{pmatrix} \vec{J}^n_{ijk} \\ \vec{M}^n_{ijk} \end{pmatrix} = - \begin{pmatrix} \vec{E}^n_{ijk} \\ \vec{H}^n_{ijk} \end{pmatrix}_{inc} - \sum_{n'}^{n-1} \sum_{i'j'k''} \times \begin{pmatrix} \varepsilon[G_{ej}]^{n-n'}_{i-i'j-j'k-k'} & \varepsilon[G_{em}]^{n-n'}_{i-i'j-j'k-k'} \\ \mu[G_{hj}]^{n-n'}_{i-i'j-j'k-k'} & \mu[G_{hm}]^{n-n'}_{i-i'j-j'k-k'} \end{pmatrix} \cdot \begin{pmatrix} \vec{J}^{n'}_{i'j'k'} \\ \vec{M}^{n'}_{i'j'k'} \end{pmatrix}. \quad (37)$$

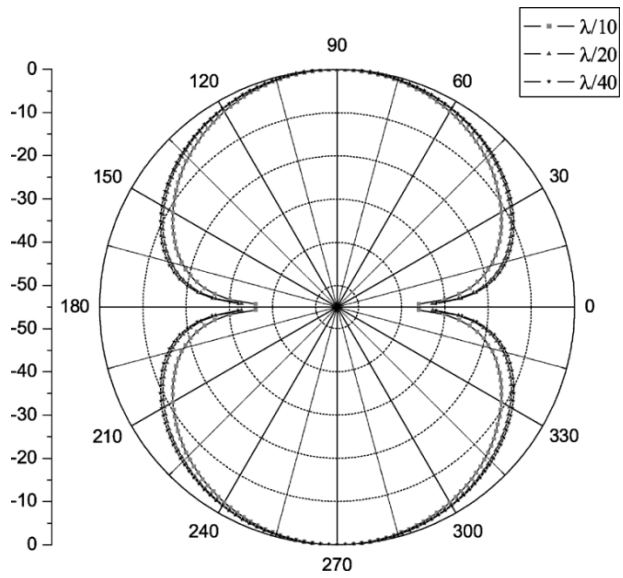

Fig. 2. Power pattern of a $\lambda/2$ dipole with the grid resolution of $\lambda/10$, $\lambda/20$, and $\lambda/40$.

When applying (37) in antenna modeling, it is maintained that the relative positions of the electric and magnetic currents follow the same distribution as the electric and magnetic fields in the Yee algorithm. The space and time steps also follow the same Courant condition as the FDTD method. The reason for this is because the DGF is based on the FDTD grid and equations. Therefore, the same resolution can be chosen for the DGF method as for the Yee algorithm. Fig. 2 shows the power pattern of a half-wavelength dipole obtained at a resolution of $\lambda/10$, $\lambda/20$, and $\lambda/40$, respectively. It is observed that the $\lambda/20$ and $\lambda/40$ results overlap each other, which shows that the DGF converges very well. It is well known that in the traditional FDTD method, results can be improved by reducing the cell sizes to produce better modeling of an antenna or scatter. While no exact rule exists for the minimum cell size, a rule of thumb of no cell's being larger than $\lambda/10$ is generally accepted. For the DGF approach, the same principle applies and since the method is derived directly from the FDTD equations, it can be deduced that the same rule of thumb will apply. However, it has been noticed that by combining with fast Fourier transform, the resolution used in the DGF method can actually decrease to Nyquist interval. This happens for the case of DGF as ABCs, which will not be discussed in detail here.

C. The Modeling of a Yagi–Uda Array

DGF-FDTD is applied to the modeling of a 15-element Yagi–Uda array. The reflector is positioned 0.15λ away from the driven element and has a length of 0.7λ and the driven element has a length of 0.5λ. Thirteen directors each of length 0.4λ are evenly spaced with an element spacing of 0.35λ. The first director is also set at a distance of 0.35λ away from the driven element. Figs. 3 and 4, respectively, are the E-plane and H-plane power patterns for the 15-element Yagi–Uda array at 300 MHz. Numerical results from NEC are also shown in the same graphs for the purpose of comparison. It is seen from these graphs that the number of lobes in both results are the same

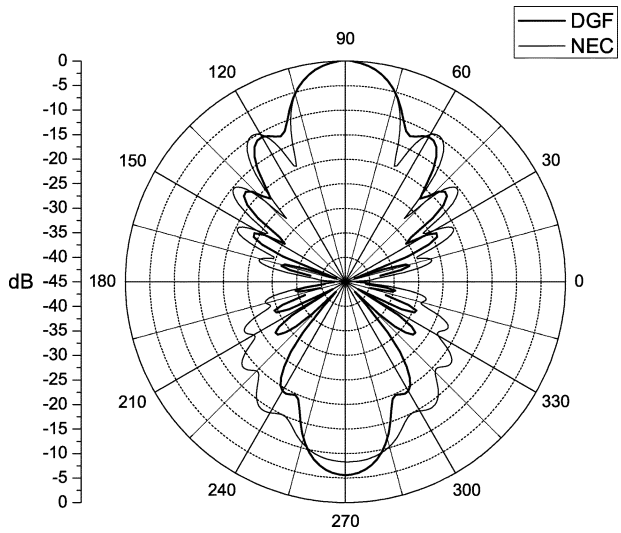

Fig. 3. E-plane power pattern of a 15-element Yagi–Uda array at 300 MHz.

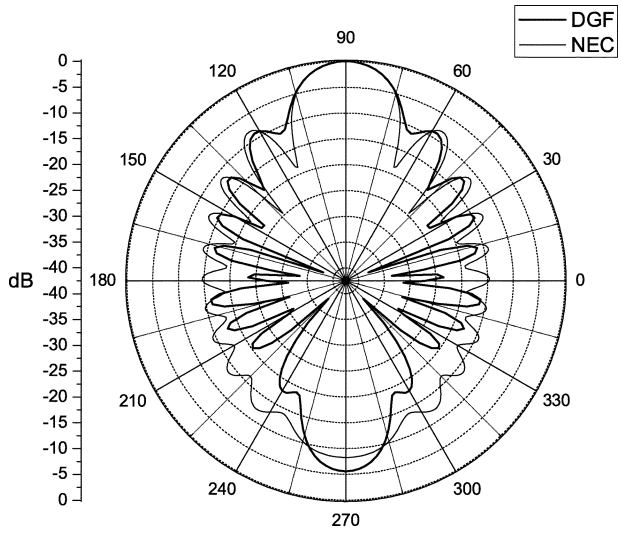

Fig. 4. H-plane power pattern of a 15-element Yagi–Uda array at 300 MHz.

and that the main lobes from both DGF and NEC overlap each other while there is a slight difference between the side lobes and a larger difference between the back lobes. The reasons for the discrepancy are, first, the frequency resolution of the postprocessing code which decides the available frequencies depends on the number of time steps and the spatial steps used in the main program; secondly, the DGF code has an inherent zero wire radius. Better agreement can be achieved by padding the raw data file with zeros and run in the fast Fourier transform for a larger number of time steps.

D. Computational Complexity

For the traditional FDTD method, the number of nodal field points in the spatial grid increases with D^3, where D is the spatial dimension of the structure, while the number of time steps needed for convergence increases linearly. Combining these features together, the net run time for FDTD will increase as D^4. For the method of moments with large problems the run time will be dominated by the solution of the linear equation set. The

matrix size N will be equal to the number of wire segments, and this will vary with D^2. For all numerical methods (NEC uses Gaussian elimination), the time needed to obtain the linear equation solution or invert the matrix will, in the limit, vary with N^3, so that the overall run time will vary with D^6.

The recorded computation time for the 15-element Yagi–Uda array using the DGF-FDTD method is approximately 3 min when run on a PIII 733 MHz desktop, which is almost as fast as NEC, but a five times improvement over the 15 min taken when using XFDTD (a commercial FDTD package), which uses the classic FDTD formulation. This significant improvement in computational time using DGF-FDTD method will help to increase the efficiency of the traditional FDTD method greatly when the two methods work together as a hybird method, which will be investigated in further papers.

IV. Conclusion

The analytical formulation of the discrete Green's function formulation of the FDTD method has been deduced for the 1-D, 2-D, and 3-D cases. The DGF formulation of the FDTD equations can determine the field value at any grid point and time step directly. As a result it does not require the computation of free-space nodes and the need for ABCs. The use of the DGF technique in advanced FDTD applications has some potentially significant benefits. It has been shown that a single boundary point at which DGF can be applied as an ABC has similar performance to a ten-layer perfectly matched layer. By studying a Yagi–Uda array, it is also shown that the DGF method can lead to savings in memory. More promising applications of the DGF method can be taken as future work.

References

[1] A. Taflove, *Computational Electrodynamics: The Finite-Difference Time-Domain Method*. Reading, MA: Artech House, 1995.

[2] K. S. Yee, "Numerical solution of initial boundary value problems involving maxwell's equation in isotropic media," *IEEE Trans. Antennas Propag.*, vol. AP-14, p. 302, 1966.

[3] M. Krumpholz and L. P. B. Katehi, "MRTD: new time-domain scheme based on multiresolution analysis," *IEEE Trans. Antennas Propag.*, vol. 44, pp. 555–571, Apr. 1996.

[4] J. M. Johnson and Y. Rahmat-Samii, "MR/FDTD: Multiple region finite difference time domain method," *Microwave Opt. Technol. Lett.*, Feb. 1997.

[5] J. Vazquez and C. G. Parini, "Discrete green's function formulation of FDTD method for electromagnetic modeling," *Electron. Lett.*, vol. 35, no. 7, pp. 554–555, Apr. 1999.

[6] J. G. Proakis and D. G. Manolakis, *Digital Signal Processing: Principles, Algorithms, and Applications*. New York: Macmillan, 1992.

[7] T. Chen-To, *Dyadic Green Functions in Electromagnetic Theory*. New York: IEEE Press, 1993.

[8] D. M. Sullivan, "Z transform theory and the FDTD method," *IEEE Trans. Antennas Propag.*, vol. 44, pp. 28–34, 1996.

[9] C. A. Balanis, *Advanced Engineering Electromagnetics*. New York: Wiley, 1989.

[10] G. Boole, *A Treatise on the Calculus of Finite Differences*. London, U.K.: Macmillan, 1880.

[11] M. Abramowitz and I. Stegun, *Handbook of Mathematical Functions*. New York: Dover, 1965.

[12] J. Stratton, *Electromagnetic Theory*. New York: McGraw-Hill, 1940.

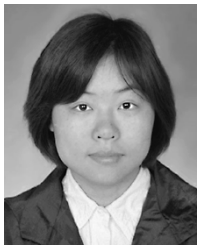

Weili Ma was born in China in 1976. She received the B.S. and M.S. degrees in electronic engineering from Beijing University of Aeronautics and Astronautics, China, in 1997 and 2000, respectively. She is currently pursuing the Ph.D. degree at Queen Mary College, University of London, U.K.

Since 2000, she has been involved in research work on the discrete Green's function formulation of the finite-difference time-domain method at Queen Mary College.

Mark R. Rayner (M'03) was born in London, U.K., in 1970. He received the B.Eng. (honors) and Ph.D. degrees from Queen Mary College, University of London, in 1991 and 1995 respectively.

Since 1995, he has been with Queen Mary College, University of London, as both a Research Assistant and a Lecturer. There, he has been involved in research in the areas of compact antenna test ranges and computational electromagnetics, most notably the finite-difference time-domain method.

Dr. Rayner is a member of the Institution of Electrical Engineers.

Clive G. Parini (M'96) received the B.Sc.(Eng.) and Ph.D. degrees from Queen Mary College, University of London, U.K., in 1973 and 1976, respectively.

He joined ERA Technology Ltd., U.K., working on the design of microwave feeds and offset reflector antennas. In 1977, he returned to Queen Mary College and is currently Professor of antenna engineering and Head of both the Communications Research Group and the Antenna and Electromagnetics Laboratory, where there is strong emphasis on EM modeling using a variety of methods including physical optics, geometric optics, GTD/UTD, method of moments, modal matching, FDTD, and numerical optimization. He has published more than 100 papers on research topics including array mutual coupling, array beam forming, antenna metrology, microstrip antennas, millimeter-wave compact antenna test ranges, and millimeter-wave integrated antennas. He is currently the Chairman of the Institution of Electrical Engineers (IEE) Antennas and Propagation Professional Network Executive Team and an Honorary Editor of the *IEE Proceedings on Microwaves, Antennas and Propagation.* He has been on the organizing committee for a number of international conferences. In 1991 he was Vice Chairman and in 2001 Chairman of the IEE International Conference on Antennas and Propagation.

Prof. Parini is a Fellow of the Institution of Electrical Engineers. In January 1990 he was one of three coworkers to receive the Institution of Electrical Engineers Measurements Prize for work on near-field reflector metrology.